SiO$_x$ protective film thermally evaporated downwards for 2-m level primary mirror

Wenjun Pei (裴文俊)* and **Hongxiang Liu (刘洪祥)****

Institute of Optics and Electronics, Chinese Academy of Sciences, Chengdu 610209, China

*Corresponding author: Peiwenjun1208@163.com; **corresponding author: hxliu123@yahoo.com.cn*

The service life of the large primary mirror with aluminum coating can be effectively prolonged by a protective layer. The SiO$_x$ (1<x<2) protective material which is thermally evaporated from up to bottom is studied. Environmental adaptability experiment, spectral measurement and micro-morphology analysis are executed on bare SiO$_x$ coatings within different oxygen concentrations, and the repeatability verification is implemented by testing the SiO$_x$ protected aluminum coatings. The results show that the SiO$_x$ coatings can meet the protective qualification within oxygen flow of 50 sccm (p=5.6×10^{-3} Pa). The fine compactness of the coating has excellent moisture resistance with the average molecular spacing of 0.335 nm. In addition, the average reflectivity of the SiO$_x$ protected aluminum coating is 90.47% in the band 400 —2 500 nm and the coating is confirmed to have good environmental performance.

OCIS codes: 310.1515, 310.6870.

doi: 10.3788/COL201311.S10214.

About 5–10 nm alumina film which makes the reflective coating a certain resistance to damage will be formed on the surface of bare aluminum reflective coating in the air[1]. However, in practical applications, this naturally formed alumina protective film is fragile. In order to enhance the damage resistance and corrosion resistance to extend the aluminum coating's service life (generally 1–3 years[2]), the protective film with transparent and firm performance is needful. More frequent use of the protective materials are SiO, SiO$_x$ (SiO oxidation, 1<x<2), and SiO$_2$[3].

The 2-m level primary mirror is mainly used in the spectral band of 400–2 500 nm. In the whole process of the preparation, the mirror temperature maintains at around room temperature. In view of the deformation and evaporation security, the mirror is placed in the bottom of the vacuum chamber, being hold by 18 points flexible support, and the evaporation sources are located above, evaporating from top to bottom. In accordance with these technical requirements, we select the SiO$_x$ (1<x<2) as the protective material and bring to further study relying on the nation's largest bell-type high-vacuum coater.

The coater is installed in the peak of 3 200 m above sea level near Lijiang City, and the ultimate vacuum can meet 4.0×10^{-5} Pa. The high vacuum system equipped with two Leybold COOVAL1800 cryogenic pumps is divided into two parallel branches to exhaust. This design not only can improve the pumping speed, obtaining the desired evaporation pressure as soon as possible (two hours to reach 4.0×10^{-4} Pa), but also can ensure the reliability of equipment operation—when one branch has problems, the other branch still meets the work demands.

The material of SiO$_x$ (1<x<2) is generated from the insufficiently oxidized SiO, and it displays the performance characteristics of SiO or SiO$_2$ subject to the degree of oxidation. The SiO which has the sublimation physical property can ensure the security when evaporating from top to bottom. Evaporation sources are special molybdenum evaporation boats, sealed by the three-tier

structure, and the above two holes with lids are connected to two material store rooms, one hole below is the material exit portal (Fig. 1). The whole evaporation system consists of three evaporation boats, which are distributed with the central angle of 120° in the same ring, separately controlled by three transformers[4,5].

The vacuum chamber diameter is 3 205 mm, and the evaporation boats can be placed on the range of 0–2600 mm (without considering the influence of the glow discharge device) as well as the vertical removable region of 1 000—1 250 nm (net of about 280 mm from the mirror surface to the support base yet). By means of the simulation[6], we have learned that the non-uniform can meet the minimum value at the height of 1 250 mm and the diameter of 2 120 mm. And all the results suggest that the non-uniformity of the film is less than 17%[4].
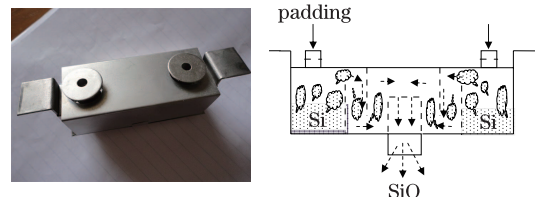

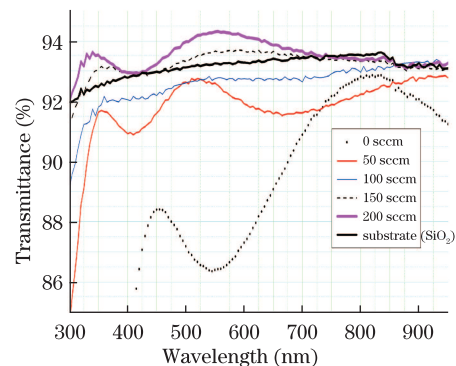Fig. 1. SiO$_x$ evaporation sources.

Fig. 2. (Color online) Transmittance of the SiO$_x$ (1<x<2) films with different oxygen flows.

Table 1. Refractive Index of Samples at $\lambda = 550$ nm

Material	SiO	SiO$_x$(1<x<2)					SiO$_2$
Oxygen Flow (sccm)	/	0	50	100	150	200	/
Refractive Index	1.55–2.0	1.7920	1.4551	1.4805	1.4357	1.3995	1.46

We have prepared a set of samples of the monolayer SiO$_x$ (1<x<2) films, the same thickness, in accordance with different oxygen flows and have tested them. Usually, in a same spectrum, the refractive index of SiO is slightly larger than that of SiO$_2$, and the refractive index of SiO$_x$(1<x<2) will tend to that of SiO$_2$ according with the intensification of the oxidation degree of SiO Be seen from Fig. 2, along with the increase of oxygen flows, the transmittance of the SiO$_x$ (1<x<2) films is generally on the increase and the refractive index decreases. Table 1 shows the refractive index of the samples with thickness of about 250 nm at $\lambda = 550$ nm, and the appearance is consistent with that of the transmission curves.

Along with the oxygen flow increasing, the pressure becomes bigger, thus the molecular free path is shortened and the chance of the molecule collision turns more, which results in the enhanced of molecular scattering and ultimately affects the film's compactness. The molecular energy is not high when thermal evaporation and the film grains exhibit an obvious columnar growth with lots of gaps. Especially long deposition distance and low surface temperature (near room temperature) make the molecular mobility very small on the surface. Thus the oxygen flow has a great influence on the film structure. Throughout all the transmission curves (greater than 1 μm, the curves are almost overlapping), the transmission curves of the samples with 150-and 200-sccm oxygen flows are higher than that of the SiO$_2$. Typically the curve of the sample with 200-sccm oxygen flow shows that the film played an apparent antireflective effect here, and it indicates that the film's refractive index is lower than that of SiO$_2$. The reason for this phenomenon is that there are so many gaps in the film that the refractive index decreases sharply after air-filled. The layers with worse compactness also play a worse role in environmental adaptability, so the film prepared with 200-sccm oxygen flow is not suitable for the protective layer.

Just from the reflectivity curves of SiO$_x$ protected aluminum films to see, all the reflectivity partly declines in the whole band (Fig. 3), especially the samples with 25-sccm oxygen flow in the visible region. Been calculated in the band 400–2 500 nm region, the average reflectivity of the sample with 25-sccm oxygen flow is about 89.74%, while the other three samples are higher than 90% (e.g., 90.47098%@50 sccm), and all of the samples meet the requirements. On the premise of good protective properties, it usually opts for the oxygen flow parameter with which the films appear high reflectivity.

The primary mirror is mainly used in the environment of 90% relative humidity, so the moisture resistance of the protective layer is particularly important. We have tested the samples of the SiO$_x$(1<x<2) films by soaking in water for 24 h. After the film gaps are filled with water, the refractive index increases, the optical thickness grows, and the spectral curve drifts to longer wavelengths. The better the compactness is, the smaller the changes of the refractive index, the optical thickness and

the spectral curve are. Because of the strong absorption near $\lambda = 300$ nm for the SiO$_x$ films by thermally evaporating SiO[7], we mainly observe the transmission from visible to infrared region. The transmitting curves of the samples, which are evaporated with different oxygen flows, before and after the soaking testing are showed in Fig. 4. The transmittances of the samples with 25-sccm oxygen flow change obviously due to lack of oxidation. And the changes of the transmittances of the samples with 50-sccm oxygen flow as well as the wavelength drift are small.

Along with the increase in the amount of oxygen, the impact of the oxygen denseness starts to become more
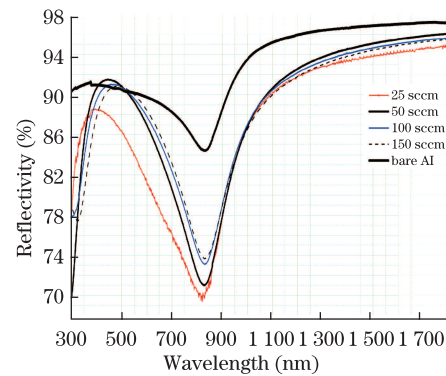

Fig. 3. (Color online) Reflectivity curves of bare aluminum film and SiO$_x$ protected aluminum films.
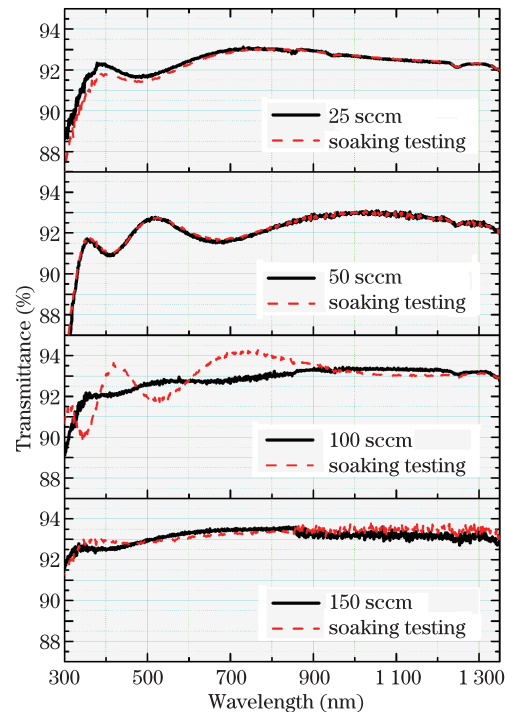

Fig. 4. (Color online) Transmittances of the samples before and after soaking testing.

apparent, the samples with 100-sccm oxygen flow have larger water absorption exist and the samples with 150-sccm oxygen flow have long wave drift increased.

We give the molecule average spacing with different oxygen flows by the X-ray diffraction (XRD) to quantify the molecular arrangement state of the thin films growth. The average molecule spacings of the samples with different oxygen flows at the same deposition rate (0.09–0.12 nm/s) are shown in Fig. 5. The average molecular spacing of the film with 50-sccm oxygen flow is smaller that of SiO film due to the high vacuum and the small oxygen partial pressure–the oxygen has less impact on the free path of the ejecting molecular clusters. And the increase of the oxygen content in a portion of the film is also a reason. With the increase in the amount of oxygen filled, it has affected the molecular free path and the molecular scattering. In the process of the film growth, we should consider the effects of the molecular migration in the horizontal direction besides that of energy in the vertical direction. The surface molecular migration in the horizontal direction is help to improve the compactness of the film. When the collision is aggravated, the energy will reduce before the particles reaching the substrate, and the surface mobility will become small. Although the particles get more oxidized, the molecular voids increase and the compactness will be weaker.

By the curves of the monolayer SiO_x films, we can conclude that it can get a better protective film with the parameters of 25- and 50-sccm oxygen flows.

The spectral curves of the aluminum reflective films with SiO_x protected before and after the high and low temperature test and the moist heat test are shown in Fig. 6(a). Compared to that before testing, the spectrum after testing changes in reflectivity less than 2%, wherein the changes of the
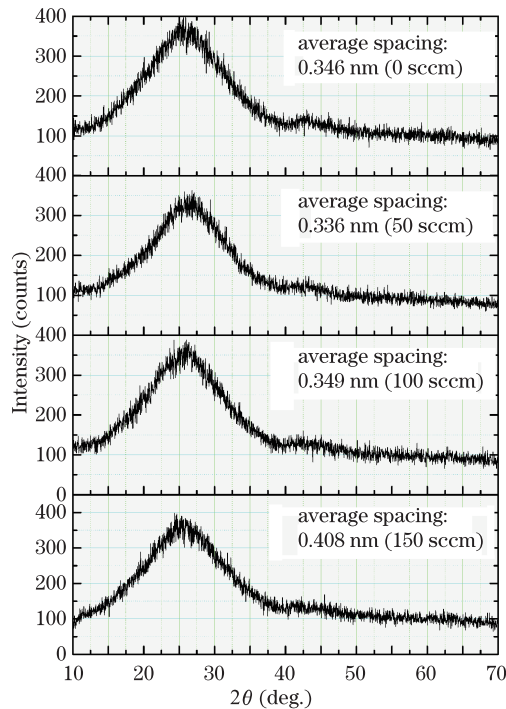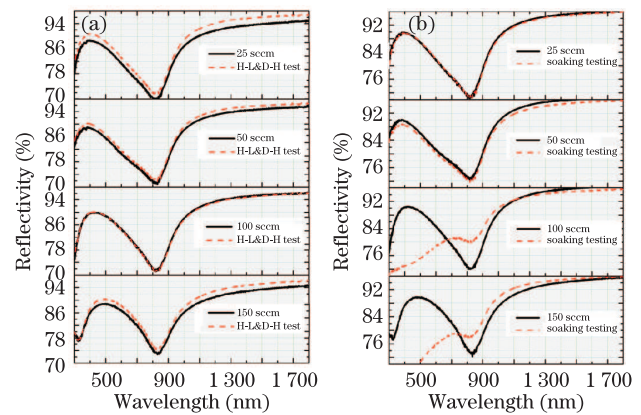

Fig. 6. Reflectivity curves before and after environmental stability test: (a) high and low temperature test; (b) 24 h soaking testing.
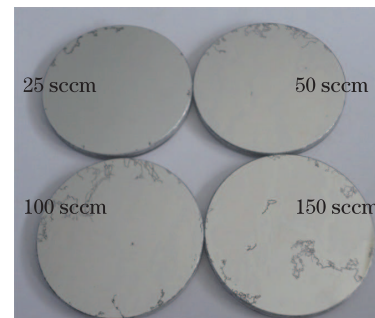

Fig. 7. Appearances of the samples after the salt spray testing.

samples with 50- and 100-sccm oxygen flows are not greater than 1%. However, the same batch of samples after 24 h soaking testing (Fig. 6(b)) show that the changes of that with 25- and 50-sccm oxygen flows are still within 2%, but the protective property of the films with the other oxygen flow parameters has been weakened or disappeared. Meanwhile we carry out the salt spray testing (5% NaCl, spraying 24 h) in accordance with the national standard on the same batch of samples, and all the samples have different degrees of corrosion, mostly on the edge (Fig. 7). In general, the corrosion areas of the samples with 25- and 50-sccm oxygen flow are smaller than others and the protective property of that is significantly.

Using the microscope to observe the surface appearance of the samples can intuitively find the reasons of the differences in former test results. By means of the microscope, 100 times, to observe the monolayer SiO_x ($1<x<2$) films before and after the soaking testing, it suggests that between the samples with 25- and 50-sccm oxygen flow, the micro-appearances are little differences, just a little bit more pinholes in the former samples. However, the samples with other oxygen flows can already see some films off, especially serious with 150-sccm.

For the SiO_x ($1<x<2$) protected aluminum coatings, the surface conditions are more clearly under the microscope, 500 times, due to the presence of the aluminum film after the soaking testing. The micro-appearances are similar to that of the monolayer SiO_x
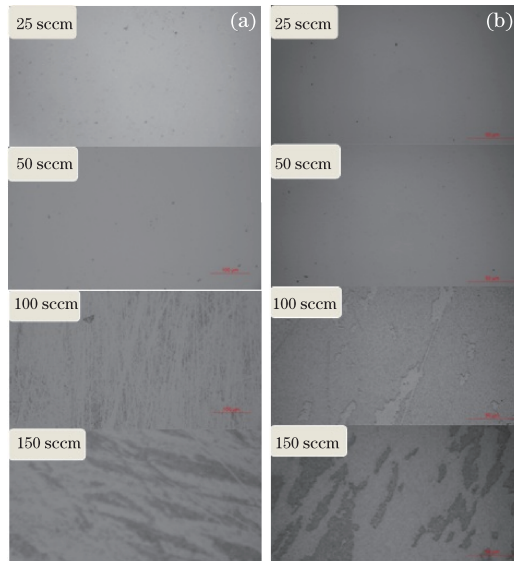

Fig. 5. Average molecule spacing testing by the XRD for SiO_x.

Fig. 8. Surface appearance of the samples by microscope after 24 h soaking testing: (a) monolayer SiO_x; (b) SiO_x protected aluminum coatings.
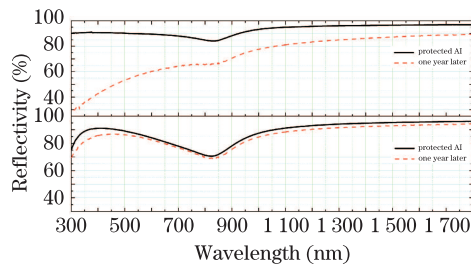

Fig. 9. (Color online) One year's timeliness test.

films with 25- and 50-sccm oxygen flows. It can obviously observe that in the samples with 100-sccm oxygen flow, parts of the protective film drop off and there are scratches by using absorbent cotton. In addition, the protective film has dropped off almost completely in the sample with 150-sccm oxygen flow. Intuitively, the surfaces of the two samples with 100- and 150-sccm oxygen flows are easily scratched when using absorbent cottons, and it suggests that they do not have any protection performance yet.

Overall, after the harsh environment stability test, only the protective films with 25- and 50-sccm oxygen flows have relatively good protection performance. Further comparison, the samples with 50-sccm oxygen flow have relatively stable performance and fewer pinholes under the microscope whether if the monolayer SiO_x films or the SiO_x protected aluminum coatings. Furthermore, it has a higher average reflectivity with the parameter of 50-sccm, so we select 50-sccm oxygen flow to prepare the protective film.

In addition, one other important factor that affects the protection performance is the evaporation rate. Increasing the evaporation rate will cause material splash, so here is mainly to study the influence on the film compactness by reducing the evaporation rate. At the evaporation rate of about 0.04 nm/s, the average molecular spacing of the sample with 50-sccm oxygen flow is 0.335 nm, the average reflectivity changes within 2% after the high and low temperature test and the damp heat test, and the corrosion area is small on the surface after the salt spray testing. All of these results are roughly the same to that at the normal evaporation rate. However, after the submerging test, the curves change larger and parts of the films drop off under the microscope. Therefore we should select the high evaporation rate to prepare the protective film in conditions that ensure safe evaporation.

The SiO_x protective film can greatly prolong the service life of the aluminum reflective coating. We select the samples of the bare aluminum coating and the SiO_x protected aluminum coating, which are prepared under the same conditions, to realize the timeliness. The two samples were placed upward in the non-enclosed room, exposed to the air. One year later, the surface of the mirror with the bare aluminum coating is scratched while wiping dust by absorbent cotton and the reflectivity has sharply decreased, especially inferior to 60% in visible region (Fig. 9). Conversely, there is no change on the surface of the mirror with the SiO_x protected aluminum coating while wiping, and the average reflectivity changes less than 4%, so the film still has a good reflective function.

In conclusion, environmental stability test and observation of surface appearances on the SiO_x ($1<x<2$) protective films with different oxygen flows suggest that the compactness and the environmental stability are good to meet the well protection performance when selecting the oxygen flow of 50-sccm to prepare the SiO_x protective film, and the average reflectivity of the protected aluminum coating can reach 90.47098% in the band 400–2 500 nm. After one year's timeliness test, the reflectivity of the unprotected reflective film declines sharply while that of the protected reflective film declines less than 4%. The results show that the service life is significantly prolonged by the protective film.

References

1. G. H. Hass and N. W. Scott, *Silicon monoxide protected front-surface mirrors* (No. AERDL-1015) (1947).
2. J. Sebag, V. L. Krabbendam, G. Poczulp, D. Neill, T. Vucina, and M. Boccas, Proc. SPIE **6273,** 62730X (2006).
3. J. T. Cox, G. Hass, and W. R. Hunter, Appl. Opt. **14,** 1247 (1975).
4. W. Du, H. Liu, W. Pei, and C. Wang, High Power Laser and Particle Beams (in Chinese) **24,** 365 (2012).
5. F. Villa and O. Pompa, Appl. Opt. **38,** 695 (1999).
6. W. Pei, H. Liu, and W. Du, Proc. SPIE **8415,** 841517 (2012).
7. D. Zhong, *Vacuum optical coatings: chooses and applications for optical material* (in Chinese) (Liaoning University Publishing Company, Shenyang, 2001) pp. 235.